UNIVERSIDADE DE SÃO PAULO

INSTITUTO DE FÍSICA
CAIXA POSTAL   20516
01000 - SÃO PAULO - SP
BRASIL

publicações

THE TIME DEPENDENT VARIATIONAL DESCRIPTION OF THE SCATTERING OF NUCLEAR FRAGMENTS[*]

by

M. Saraceno

Departamento de Física, Comisión Nacional de Energía Atómica, 1426 Buenos Aires, Argentina

The Time Dependent Variational Description of the Scattering
of Nuclear Fragments*

M. SARACENO

Departamento de Física, Comisión Nacional de Energía Atómica,
1426 Buenos Aires, Argentina

Abstract

        The Time Dependent Variational Principle is applied
to the scattering of closed shell oscillator fragments.   The
effects of antisymmetrization are included and we show how
they lead to a change in the structure of the phase space of
relative motion.   The main new feature is the appearence of
forbidden and distorted regions in phase space which have, in
the quantum treatment, a close connection with states   for-
bidden and partially allowed by the Pauli principle.The elastic
phase shifts are evaluated semiclassically in the   distorted
phase space. The method is applied in detail to the simple but
quite realistic case of $\alpha-\alpha$ scattering.

1. INTRODUCTION

        Although the Time Dependent Variational Principle
(TDVP) in quantum mechanics has a long history[1] it has only
recently been applied to realistic computations in nuclear
physics. These computations have successfully described in a
microscopic way many qualitative and also quantitative features
of the dynamics of large nuclear fragments which include deep
inelastic and fission phenomena in heavy systems and fusion
in lighter ones. This has been done in the framework of the
Time Dependent Hartree Fock (TDHF) theory where the wave func-
tion is restricted to be a Slater determinant at all times.
There is an extensive literature on this subject. Recent re-
views of both theoretical aspects[2] and numerical applications[3]
have been published and extensive reference to the original
literature is there provided.

        There are two main features in the TDHF description
of a nucleus-nucleus collision that we want to focus upon:

i) The Pauli principle is taken into account exactly.   This
   happens because the single particle states all evolve in
   the same (time dependent) field and therefore the ortho-
   gonality of the wave functions is assured at all times.

ii) The excitation of the fragments and its coupling to the
    relative motion is treated self-consistently and exactly
    (inasmuch as it can be described by one-body dynamics).
    The internal motion is not parametrized in any way and the
    only input to the calculation is the two body force (of
    Skyrme type) and the initial conditions.This allows in
    particular for a microscopic description of the large
    dissipation of kinetic energy that occurs in a deep inelastic
    collision.

As a disadvantage we should point out the lack of a practical
way to extract quantum information from the calculations and
the large amount of numerical work that goes into them. The
other microscopic methods available for the treatment of nu-
cleus-nucleus scattering are the closely related Resonating
Group Method (RGM)[4] and Generator Coordinate Method (GCM)[5].

Both approaches are entirely quantum mechanical and they are capable of providing relative motion wave functions and phase shifts. They take into account the Pauli principle exactly but in their usual application they assume that the fragments cannot be excited so that only the relative motion degree of freedom is considered. In practical applications of both RGM and GCM one is limited to rather light fragments ($A \leqslant 40$) and the complications increase very rapidly if they are not closed oscillator shells. The computation of overlap and energy kernels which provide the microscopic input to these calculations is at a very sophisticated stage and makes use of powerful mathematical techniques[6,7] (Group theory, Bargmann Space).

In a nutshell we can say that TDHF treats the coupled dynamics of the relative motion and the intrinsic degrees of freedom in a classical context without violating the Pauli principle. RGM and GCM instead only treat the relative motion, disregarding the coupling to other degrees of freedom. However, they do this quantum mechanically, also without violating the Pauli principle.

The method that we propose in this work is somehow the intersection of these two approaches. We use a trial wave function which is essentially the same as in GCM but the generator coordinate is treated as a time dependent parameter in the TDVP. With this we obtain a classical description of the relative motion which takes into account the Pauli principle (but not the coupling to other degrees of freedom). A similar method, called the Time Dependent Cluster Theory, has been proposed recently[8,9]. However, the emphasis has been in the classical solution of initial value problems much in the same spirit as in TDHF. Here we shift the emphasis to the study of the symplectic structure, or generalized phase space, associated to the norm kernel. By doing this we are able to incorporate the effects of the Pauli principle into a "distortion" of the phase space of relative motion.

Instead of solving the equations of motion and displaying trajectories we also shift the emphasis to the computation of quantities which have a quantum interpretation. These quantities, usually computed as areas in the distorted phase

space, can provide semiclassical information on bound states, resonances and phase shifts.

The presentation is organized as follows. In section 2. we give a brief overview of the TDVP especially in connection with a trial wave function parametrized analytically. In section 3. we describe the trial wave function in general terms leaving some technical details for Appendix A. In section 4. we study the symplectic structures associated to the interaction of SU(3) scalar fragments and we show how the Pauli principle appears in classical phase space. In section 5. we apply the method to the simple but still quite realistic case of α-α scattering. We show how to evaluate the elastic phase shifts from the variational equations and compare them to the RGM computation of Okai and Park[10].

2. THE TDVP WITH COMPLEX PARAMETERS

Recently, we have studied the structure and the geometry of the TDVP in quantum mechanics especially in relationship with Lie groups and symplectic structures on orbits of their coadjoint representations[11]. In this section we review briefly the symplectic structure and the variational equations associated with a trial wave function parametrized analytically, regardless of the existence of such a group structure.

We assume a many body wave function $|\psi(\bar{z}_1,...,\bar{z}_r\rangle$ [*)] parametrized in terms of r complex numbers z_i. Their physical significance depends on the problem at hand and they usually measure some geometrical property whose approximate time dependence one wishes to describe. We assume that $|\psi\rangle$ depends analytically on $\bar{z}$. This means that the dependence is only on $\bar{z} = \mathrm{Re}\, z - i\, \mathrm{Im}\, z$, and not on z. This requirement is violated if the wave function is normalized so that we will not assume a

---

*) The bar denotes complex conjugation. The use of $\bar{z}$ in the ket wave function is conventional. When no confusion is possible we will abbreviate $|\psi(\bar{z}_1,...,\bar{z}_r)\rangle = |z\rangle$

definite normalization. Accordingly, the usual[12] TDVP is modified to make the action, and therefore the equations of motion, invariant under a change of phase or normalization of the wave function. This is achieved by defining the action as

$$S = \int L \, dt \qquad (2.1)$$

where the quantum Lagrangian is given by

$$L = \frac{i\hbar}{2} \cdot \frac{\langle\psi|\dot{\psi}\rangle - \langle\dot{\psi}|\psi\rangle}{\langle\psi|\psi\rangle} - \frac{\langle\psi|H|\psi\rangle}{\langle\psi|\psi\rangle} \qquad (2.2)$$

the bracket indicates integration over coordinates, spin and isospin of all particles and H is the microscopic hamiltonian. It is well known[11,12] that unrestricted variation of (2.1) leads to the time dependent Schrödinger equation while variations compatible with a given parametrization yield equations of motion of a classical nature for the variational parameters. Using the parametrized wave function we obtain

$$L = \frac{i\hbar}{2} \sum_{i=1}^{r} \left(\dot{\bar{z}}_i \frac{\partial}{\partial \bar{z}_i} - \dot{z}_i \frac{\partial}{\partial z_i} \right) \ln N - H \qquad (2.3)$$

Once a trial wave function is chosen the ingredients needed to compute the action are then the norm and the energy

$$N(z,\bar{z}) = \langle z|z\rangle \qquad (2.4)$$

$$H(z,\bar{z}) = \frac{\langle z|H|z\rangle}{\langle z|z\rangle} \qquad (2.5)$$

Variation of the action with the lagrangian (2.3) yields the equations of motion

$$i\hbar \sum_j g_{ij} \dot{\bar{z}}_j = \frac{\partial H}{\partial z_i} \quad , \quad \text{and} \quad \text{c.c.} \qquad (2.6)$$

where

$$g_{ij} = \frac{\partial^2}{\partial z_i \partial \bar{z}_j} \ln N \qquad (2.7)$$

The matrix g_{ij}, which is determined completely once the norm of the trial wave function is known, will be of paramount importance for our discussion in Section 4.

The symplectic structure associated to the parametrization is revealed by defining a Poisson bracket for general function $F(z,\bar{z})$, $G(z,\bar{z})$

$$\{F,G\} = \sum_{i,j=1}^{r} \left\{ \frac{\partial F}{\partial \bar{z}_i} g_{ij}^{-1} \frac{\partial G}{\partial z_j} - \frac{\partial G}{\partial \bar{z}_i} g_{ij}^{-1} \frac{\partial F}{\partial z_j} \right\} \qquad (2.8)$$

In particular we obtain the fundamental brackets

$$\{\bar{z}_i, z_j\} = g_{ij}^{-1}$$
$$\{z_i, z_j\} = \{\bar{z}_i, \bar{z}_j\} = 0 \qquad (2.9)$$

and the equations of motion

$$i\hbar \, \dot{\bar{z}}_i = \{\bar{z}_i, H\} \quad \text{and} \quad \text{c.c.} \qquad (2.10)$$

The Poisson bracket form of these equations assure the energy conservation along the solution trajectories. The main advantage of defining the lagrangian as in (2.2) is that then the equations of motion are independent of the phase and normalization chosen for the wave function. The proper phase and norm[13], as specified by the time dependent Schrödinger equation, are restored by

$$|\Phi(t)\rangle = e^{iS} \frac{|z(t)\rangle}{\sqrt{\langle z|z\rangle}} \qquad (2.11)$$

where S is the action (2.1) computed for a given trajectory $z(t)$.

An important special case occurs when the norm is given by

$$N = \exp\left[\sum_{i=1}^{r} \bar{z}_i \, z_i \right] \qquad (2.12)$$

In that case $g_{ij} = \delta_{ij}$; (cf. (2.7)) and the symplectic structure is the usual canonical Poisson bracket. If real and imaginary parts of z are defined as $z_i = 1/\sqrt{2\hbar} \, (q_i - ip_i)$ the action becomes the usual one in classical mechanics[14)]

$$ S = \int \left[\sum_{i=1}^{r} p_i \dot{q}_i - H \right] dt $$

We will refer to this case as canonical and call the associated phase space flat.

3. THE TRIAL WAVE FUNCTION

As in all variational calculations, the family of wave functions to be used in the TDVP will depend partly on our physical insight into a given situation and partly on questions of mathematical convenience. Our main assumption will be that the scattering of two nuclear fragments can be described by a trial wave function which is a totally antisymmetrized product of single particle states centered at two different positions and boosted so as to have different momenta. The second assumption is that the fragments remain unexcited during the collision so that only the relative motion degree of freedom is taken into account and its dynamics investigated. A third assumption, more technical in nature and which simplifies matters considerably, is to assume oscillator states of the same frequency in both fragments. The trial wave function is constructed from single particle states $|i_1)$, $i_1 = 1,\ldots,A_1$ in one fragment and $|i_2)$, $i_2 = 1,\ldots,A_2$ in the other. The label i stands for all the quantum numbers (n,ℓ,m,s,t) needed to specify the single particle state. As we describe in more detail in Appendix A the displaced and boosted fragments are constructed from states

$$ |i_1,\underline{s}) = \exp\left[\frac{\sqrt{\mu}}{A_1} \, \underline{s}.\hat{\underline{a}}^\dagger \right] |i_1) \quad \text{in fragment 1} $$

$$ |i_2,\underline{s}) = \exp\left[-\frac{\sqrt{\mu}}{A_2} \, \underline{s}.\hat{\underline{a}}^\dagger \right] |i_2) \quad \text{in fragment 2} $$

$$(3.1)$$

where $|i)$ are oscillator states and $\hat{\underline{a}}^\dagger$ the corresponding creation operator. The complex vector $\underline{s}$, which we take as the variational parameter, is related to the relative distance $\underline{Q}$ and momentum $\underline{P}$ of the centers of mass of the fragments by

$$ \underline{s} = \frac{1}{\sqrt{2}} \left[\frac{\sqrt{\mu} \, \underline{Q}}{b} - \frac{b\underline{P}}{\hbar\sqrt{\mu}} \right] \tag{3.2} $$

Here $b = \sqrt{\hbar/(m\omega)}$ is the oscillator lenght and $\mu = A_1 A_2 / (A_1 + A_2)$ is the relative mass number. The trial wave function is then

$$ |\underline{s}> = A\left[\prod_{i_1=1}^{A_1} |i_1,\underline{s}) \prod_{i_2=1}^{A_2} | i_2,\underline{s}) \right] \tag{3.3} $$

We refer to Appendix A for notation and a more detailed analysis of the construction of this wave function. Here we want to stress some properties that are important for our further discussion.

a) In any representation $|\underline{s}>$ is an A×A ($A = A_1 + A_2$) Slater determinant. It is built up from non-orthogonal and non-normalized single particle states which are parametrized analytically by the complex vector $\underline{s}$.

b) $|\underline{s}>$ does not have in general a well defined linear momentum. However the fact that we use oscillator states of the same frequency in both fragments leads to the well known fact[15)] that the CM coordinate separates in a product wave function completely uncoupled from the relative motion. If we do not use oscillator states (as in most TDHF calculations) or even if the fragments have unequal frequencies then the CM does not separate. In any case, however the mean values of the CM coordinates and momenta are zero.

c) The angular momentum is also not a good quantum number for $|\underline{s}>$. A classical angular momentum can be associated to a given $\underline{s}$ by

$$ \underline{L} = \frac{1}{\hbar} \, \underline{R} \times \underline{P} = i \, \bar{\underline{s}} \times \underline{s} \tag{3.4} $$

This is a classical quantity and can take any continuous value. However it can only be used as a conserved angular momentum in the asymptotic region where the clusters do not overlap. We return to this question in Section 5.

There are well known projection methods to obtain states which have a well defined linear and angular momentum from Slater determinants which do not. They usually involve large computational efforts which for the moment we wish to avoid. We will therefore in what follows treat the angular momentum as a classical quantity.

4. SYMPLECTIC STRUCTURES ASSOCIATED TO THE INTERACTION OF SU(3) SCALAR FRAGMENTS

Although the trial wave function $|s>$ is quite general we will consider here only the case in which both fragments are closed shell oscillator wave functions with the same frequency. This is the simplest case because then the isolated fragments are spherically symmetric and SU(3) invariant and all computations can be done analytically. In practice this restricts the direct application of the method to ^4He, ^{16}O and ^{40}Ca as interacting clusters. However the picture that emerges is general and the restriction to SU(3) invariance or equal frequency can be lifted at the expense of a substantial increase in complexity.

4.1. The symplectic structure

We apply the general connection between the overlap and the symplectic structure, embodied in (2.7), to the trial states constructed in Section 3. Explicit formulas for the overlap for some pairs of fragments are given in (A.25) to (A.28). In all cases $<s|s>$ can be written as

$$<s|s> = N(\underline{s}.\bar{\underline{s}}) = \exp(\underline{s}.\bar{\underline{s}})\left[M(\underline{s}.\bar{\underline{s}})\right]^4 \qquad (4.1)$$

where the fact that the overlap depends only on the scalar $\underline{s}.\bar{\underline{s}}$ (and not on $\underline{s}.\underline{s}$ or $\bar{\underline{s}}.\bar{\underline{s}}$) is a direct consequence of the SU(3) invariance.

The matrix g that defines the symplectic structure is easily computed from (2.7) and (4.1)

$$g_{ij} = \frac{\partial \ln N}{\partial s_i \partial \bar{s}_j} = \delta_{ij} u + \bar{s}_i s_j v \qquad (4.2)$$

where

$$u = \frac{\partial \ln N}{\partial(\underline{s}.\bar{\underline{s}})} = 1 + 4\frac{\partial \ln M}{\partial(\underline{s}.\bar{\underline{s}})} \qquad (4.3)$$

$$v = \frac{\partial^2 \ln N}{\partial(\underline{s}.\bar{\underline{s}})^2} = 4\frac{\partial^2 \ln M}{\partial(\underline{s}.\bar{\underline{s}})^2} \qquad (4.4)$$

Asymptotically, for $\underline{s}.\bar{\underline{s}} \to \infty$, we have $u \to 1$ and $v \to 0$ and therefore g becomes the unit matrix. As a sum of a diagonal and a separable matrix g is easily inverted

$$(g^{-1})_{ij} = u^{-1}\left[\delta_{ij} - \frac{v}{u + \underline{s}.\bar{\underline{s}} v} \bar{s}_i s_j\right] \qquad (4.5)$$

The symplectic bracket for arbitrary functions is then defined according to (2.8)

$$\{F,G\} = \sum_{i,j=1}^{3}\left(\frac{\partial F}{\partial \bar{s}_i}(g^{-1})_{ij}\frac{\partial G}{\partial s_i} - \frac{\partial G}{\partial \bar{s}_i}(g^{-1})_{ij}\frac{\partial F}{\partial s_j}\right)$$

$$(4.6)$$

In particular

$$\{\bar{s}_i,s_j\} = (g^{-1})_{ij}$$

$$(4.7)$$

$$\{s_i,s_j\} = \{\bar{s}_i,\bar{s}_j\} = 0$$

In principle this is all we need to solve the equations of motion, which are given by

$$i\hbar \; \dot{\bar{s}}_i = \{\bar{s}_i, H\} \qquad (4.8)$$

Numerical solutions can be easily obtained from given initial conditions, as is done, for example in ref.[8]. However it is more convenient to first rewrite (4.8) in terms of canonical variables so that all the results of classical two body scattering can be utilized.

The transformation to canonical variables, which of necessity will itself be non-canonical, is guaranteed to exist locally for any symplectic manifold (this is known as Darboux theorem[16]). In the next section we construct it explicitly for all points of the manifold. The distinct new feature that emerges is the appearance of boundaries which exclude certain regions in phase space. We will show that these regions can be directly linked to states which in the quantum treatment are excluded by the Pauli principle.

4.2. Transformation to canonical variables

The easiest way to find the canonical variables is to go back to the action (2.1) (without the energy term)

$$S_0 = \frac{i\hbar}{2} \int dt \; \sum_{i=1}^{3} \; (\dot{\bar{s}}_i \frac{\partial}{\partial \bar{s}_i} - \dot{s}_i \frac{\partial}{\partial s_i}) \; \ln N \qquad (4.9)$$

Using the fact that N is only a function of $\underline{s}.\underline{\bar{s}}$ we rewrite (4.9) as

$$S_0 = \frac{i\hbar}{2} \int dt \; (\dot{\underline{\bar{s}}}.\underline{s} - \dot{\underline{s}}.\underline{\bar{s}}) \; u$$

where u is given by (4.3). It is then easy to check that the new variables

$$\begin{aligned} \omega_i &= \sqrt{u} \; s_i \\ \bar{\omega}_i &= \sqrt{u} \; \bar{s}_i \end{aligned} \qquad (4.10)$$

transform S_0 into

$$S_0 = \frac{i\hbar}{2} \int dt \; (\dot{\underline{\bar{\omega}}}.\underline{\omega} - \dot{\underline{\omega}}.\underline{\bar{\omega}}) \qquad (4.11)$$

The variables ω_i are then canonical in the sense that

$$\{\bar{\omega}_i, \omega_j\} = \delta_{ij} \qquad (4.12)$$

$$\{\bar{\omega}_i, \bar{\omega}_j\} = \{\omega_i, \omega_j\} = 0$$

This is obvious from (4.11) and can also be checked directly using the explicit expression for the bracket given in (4.6).

In terms of $\underline{\omega}$ the variational equations take the canonical form

$$i\hbar \; \dot{\bar{\omega}}_i = \frac{\partial H}{\partial \omega_i} \quad \text{and c.c.} \qquad (4.13)$$

where H is assumed to be expressed as a function of $\underline{\omega}$ by inversion of (4.10). To make these equations appear even more familiar we can transform to real variables defined in analogy to (3.2)

$$\underline{\omega} = \frac{1}{\sqrt{2}} \left[\frac{\sqrt{\mu} \; \underline{r}}{b} - i \frac{b \; \underline{p}}{\sqrt{\mu} \; \hbar} \right] \qquad (4.14)$$

where $\underline{r} = u^{1/2} \underline{Q}$ and $\underline{p} = u^{1/2} \underline{P}$.

In terms of $\underline{r}$, $\underline{p}$ everything looks like ordinary classical hamiltonian mechanics i.e.

$$\dot{\underline{r}} = \{\underline{r}, H\} \qquad \dot{\underline{p}} = \{\underline{p}, H\}$$

$$\{r_i, p_j\} = \delta_{ij} \qquad (4.15)$$

In (4.15) a factor $1/i\hbar$ has been absorbed in the bracket to conform to the standard definition of the Poisson bracket in classical mechanics.

The important new feature is that, while $\underline{Q}$ and $\underline{P}$ could assume all possible values, the canonical pair $\underline{r}, \underline{p}$ has boundaries, i.e. some regions of phase space are not allowed. To study these boundaries we go back to complex variables. From (4.10) we obtain

$$\underline{\omega}.\bar{\underline{\omega}} = \underline{s}.\bar{\underline{s}} \ u(\underline{s}.\bar{\underline{s}}) \qquad\qquad (4.16)$$

The function $\underline{\omega}.\bar{\underline{\omega}}$, which for reasons that will be clear below will be called the Pauli distortion factor, can be computed explicitly using (4.3) and the expressions for the overlap given in Appendix A. It has been plotted for several combinations of fragments in Fig. 1. Some general characteristics of this function are worth noticing. For $\underline{s}.\bar{\underline{s}} \to \infty$, $\underline{\omega}.\bar{\underline{\omega}} \to \underline{s}.\bar{\underline{s}}$. In this region the $\underline{s}$ variables themselves are canonical and the Pauli principle inoperative. For convenience we define a number N_f such that for $\underline{\omega}.\bar{\underline{\omega}} > N_f$, $\underline{\omega}.\bar{\underline{\omega}}$ differs from $\underline{s}.\bar{\underline{s}}$ by less than 1%. We call this the folding region. At the other extreme we see that for $\underline{s}.\bar{\underline{s}} \to 0$ we obtain for $\underline{\omega}.\bar{\underline{\omega}}$ a definite non-zero number N_0 characteristic of the pair of fragments. The region $\underline{\omega}.\bar{\underline{\omega}} < N_0$ is forbidden. For values $N_0 \leqslant \underline{\omega}.\bar{\underline{\omega}} < N_f$ there is a large difference between $\underline{\omega}.\bar{\underline{\omega}}$ and $\underline{s}.\bar{\underline{s}}$ but the region is allowed. The canonical phase space ω can then be divided in three regions as follows

$$N_f < \underline{\omega}.\bar{\underline{\omega}} \quad \text{folding region}$$

$$N_0 \leqslant \underline{\omega}.\bar{\underline{\omega}} < N_f \quad \text{Pauli distorted region} \qquad (4.17)$$

$$\underline{\omega}.\bar{\underline{\omega}} < N_0 \quad \text{Pauli forbidden region}$$

In table 1 we give the values N_0 and N_f for some pairs of SU(3) scalar fragments. If the antisymmetrization between fragments

	$\alpha-\alpha$	$\alpha - {}^{16}0$	$\alpha - {}^{40}Ca$	${}^{16}0 - {}^{16}0$
N_0	4	8	12	24
N_f	10	21	30	80

Table 1: Boundaries between forbidden, distorted, and folding regions (as defined by (4.17)) of the canonical phase space for the interaction of some SU(3) scalar fragments. N_f has been determined at the point where $u = 1.01$.
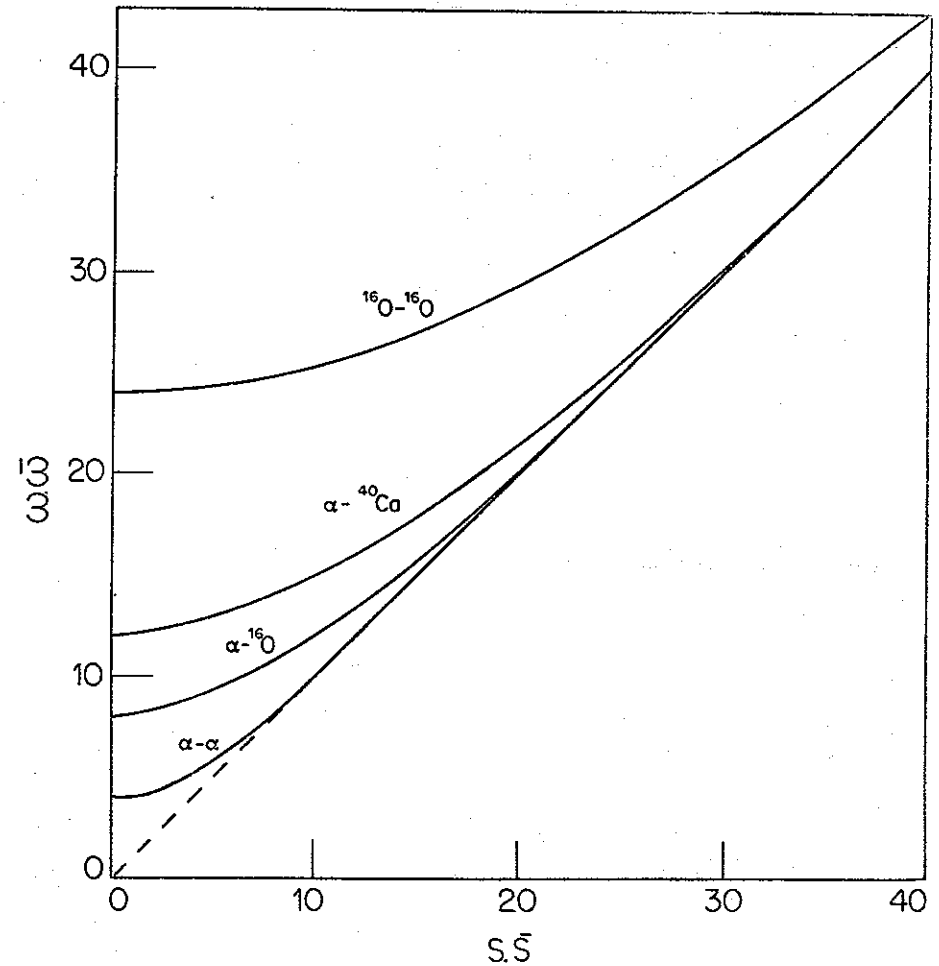
Figure 1 - Pauli phase space distortion factor for some combination of SU(3) scalar fragments. The dotted line corresponds to the neglect of antisymmetrization.

were omitted the trial wave function would be a product of two Slater determinants and the factor M in (4.1) would be equal to 1. Then $u=1$ and $\underline{\omega}$ would be equal to $\underline{s}$ throughout their ranges. In Fig. 1 we have drawn this as a dotted line. Deviations from this line reflect the effects of the Pauli principle and start becoming noticeable for $\underline{\omega}.\bar{\underline{\omega}} \lesssim N_f$. The reason for calling $\underline{\omega}.\bar{\underline{\omega}} > N_f$ the folding region comes from the fact that when antisymmetrization is neglected the potential energy between the clusters is obtained by folding the density of each one with the two body force. This is a procedure that has been used extensively to compute the real part of optical potentials between heavy ions[17]. Our considerations make a definite prediction as to the region of phase space where neglecting antisymmetrization is a valid assumption.

4.3. Radial coordinates and forbidden regions

To see more clearly the meaning of the different regions discussed in the previous section we introduce radial variables. We define as usual

$$r = (\underline{r}.\underline{r})^{1/2} = \frac{b}{\sqrt{\mu}} \left[\underline{\omega}.\bar{\underline{\omega}} + \frac{1}{2} (\bar{\underline{\omega}}.\bar{\underline{\omega}} + \underline{\omega}.\underline{\omega}) \right]^{1/2}$$

$$k = \frac{\underline{r}.\underline{p}}{\hbar r} = \frac{1}{2ir} \left[\underline{\omega}.\underline{\omega} - \bar{\underline{\omega}}.\bar{\underline{\omega}} \right] \qquad (4.18)$$

$$\ell^2 = \hbar^{-2} |\underline{r} \times \underline{p}|^2 = (\omega.\bar{\omega})^2 - (\underline{\omega}.\underline{\omega})(\bar{\underline{\omega}}.\bar{\underline{\omega}})$$

The second part of the identities have been obtained using (4.14). Instead of the radial momentum p_r we use the more convenient radial wave number $k = p_r/\hbar$. These formulas provide the transformation from the scalar quantities $\underline{\omega}.\bar{\underline{\omega}}$, $\underline{\omega}.\underline{\omega}$ and $\bar{\underline{\omega}}.\bar{\underline{\omega}}$ to the radial phase space variables r, k and the angular momentum ℓ. Using (4.14) and (4.15) we obtain

$$\underline{\omega}.\bar{\underline{\omega}} = \frac{1}{2} \left[\mu \frac{r^2}{b^2} + \frac{b^2}{\mu} (k^2 + \ell^2/r^2) \right] \qquad (4.19)$$

We will see below that ℓ is the conserved angular momentum. So it makes sense to consider the curves $\underline{\omega}.\bar{\underline{\omega}} = N$ in the radial phase plane (k,r) for fixed ℓ. They are closed curves which decrease in size as ℓ becomes larger and disappear altogether for $\ell > N$. The forbidden region $\underline{\omega}.\bar{\underline{\omega}} < N_0$ will then appear as a hole in the radial phase space for $\ell < N_0$. For $N_0 < \ell < N_f$ there is no forbidden region but there will still be a distortion region where there is an effect of the Pauli principle. For $\ell > N_f$ the interaction will be governed by the local folding potential and antisymmetrization will be irrelevant. Examples of these radial phase spaces with the different regions are given in Fig. 2 for the case of α-α scattering.

4.4. Relationship with quantum results

There is a deep connection between our results based on the symplectic structure associated to the TDVP and the more familiar ones based on RGM or GCM. We will just indicate how this connection works without attempting a detailed comparison which we leave for a future publication.

It is well known[6,7] that a power series expansion of the norm kernel in the Bargmann representation give the eigenvalues and eigenfunctions of the norm operator. Thus with N expanded as

$$N = \sum_{N=N_1}^{\infty} \lambda_N \frac{(\underline{s}.\bar{\underline{s}})^N}{N!} \qquad (4.20)$$

we can read off the eigenvalues λ_N from the expansion. The interpretation of this result, which is valid for SU(3) scalar fragments, is to say that the eigenfunctions of the norm operator are harmonic oscillator wave functions (given here in the Bargmann representation). The eigenvalues depend only on the principal oscillator number N and are degenerate with respect to ℓ and m. This is of course a consequence of SU(3) invariance.

States of relative motion forbidden by the Pauli principle have $\lambda_N = 0$ and occur for $N < N_1$ where N_1 is characteristic of the pair of fragments considered. We now prove that N_1 is equal to N_0 as defined in (4.17). In fact we have

$$N_0 = \underline{s} \cdot \underline{\bar{s}} \; u(\underline{s} \cdot \underline{\bar{s}}) \Big|_{\underline{s} \cdot \underline{\bar{s}} = 0}$$

Using (4.3) and (4.20) we obtain

$$N_0 = \underline{s} \cdot \underline{\bar{s}} \; \frac{\partial}{\partial(\underline{s} \cdot \underline{\bar{s}})} \ln \left\{ \lambda_{N_1} \frac{(\underline{s} \cdot \underline{\bar{s}})^{N_1}}{N_1!} + \dots \right\} =$$

$$= \underline{s} \cdot \underline{\bar{s}} \; \frac{N_1 (\underline{s} \cdot \underline{\bar{s}})^{N_1 - 1} + \dots}{(\underline{s} \cdot \underline{\bar{s}})^{N_1} + \dots}$$

Then for $\underline{s} \cdot \underline{\bar{s}} \to 0$ we obtain

$$N_0 = N_1$$

Therefore the number N_0 giving the boundary of the forbidden region coincides with the first principal oscillator number not forbidden by the Pauli principle. The interpretation of N_f is also quite simple. It is known that $\lambda_N \to 1$ when $N \to \infty$. In the region where λ_N is almost unity (say to within 1%) the normalization operator is the unit operator and there is no influence from the Pauli principle. The number N_f for which this happens coincides very closely with the number derived from the symplectic structure. In the region between N_0 and N_f the eigenvalues λ_N go smoothly from zero to one and one speaks of partially forbidden states. This region corresponds to the Pauli distorted region.

Another connection is even more graphical. If one thinks of a quantum state as occupying an area $2\pi\hbar$ in phase space, as one does in the WKB limit of quantum mechanics, then the forbidden area can be thought of as representing semiclassicaly a certain number of forbidden states. This number is easily calculated as the area (divided by 2π) enclosed by the curve

$$N_0 = \frac{1}{2} \left[\mu \frac{r^2}{b^2} + \frac{b^2}{\mu} (k^2 + \ell^2/r^2) \right]$$

for given N_0 and ℓ. This area is

$$J = 2\pi \frac{N_0 - \ell}{2}$$

Then if we consider the radial quantum number n_r ($N = 2n_r + \ell$) we see that the forbidden area corresponds exactly to the number of radial states with $n_r \leqslant \frac{1}{2}(N_0 - \ell)$ compatible with N_0 and ℓ. It is then apparent that a study of the symplectic structure reveals many of the features of the quantum treatment of the Pauli principle, but depicts them semiclassically. This can be quite significant for larger fragments where the quantum treatment of the overlap kernel becomes very cumbersome.

5. DYNAMICS

Once having ascertained the structure of the phase space appropriate for the description of the scattering of composite particles we turn to dynamical questions. Here the choice of a microscopic interaction will be crucial for a correct description. As our concern is to see how far a classical description via the TDVP can go we adopt the point of view of taking an existing calculation with a given two-body force and using it in the TDVP. For the present discussion we adopt the RGM calculation of α-α phase shifts by Okai and Park[10] as an "exact" calculation. The details of the two-body interaction and the explicit expressions for the hamiltonian kernel are given in Appendix B.

5.1. Conservation of angular momentum

The hamiltonian kernel (2.5) depends in principle on the vectors $\underline{s}$ and $\underline{\bar{s}}$. As the fragments are spherically symmetric it can only depend on the three scalar combinations $\underline{s} \cdot \underline{\bar{s}}$, $\underline{s} \cdot \underline{s}$ and $\underline{\bar{s}} \cdot \underline{\bar{s}}$. The same will happen after the transformation to canonical variables $\underline{\omega}$. The form of the hamiltonian will then be $H = H(\underline{\omega} \cdot \underline{\bar{\omega}}, \underline{\omega} \cdot \underline{\omega}, \underline{\bar{\omega}} \cdot \underline{\bar{\omega}})$. This form, together with the canonical equations (4.13) guarantees the conservation of angular momentum defined as

$$\underline{\ell} = i \underline{\bar{\omega}} \times \underline{\omega} = \frac{1}{\hbar} \; \underline{r} \times \underline{p} = \frac{\mu}{\hbar} \; \underline{Q} \times \underline{P} \tag{5.1}$$

Notice that, in the region of overlap, where $u \neq 1$, the conserved angular momentum differs from the asymptotic angular momentum. This is another manifestation of the effects of the Pauli principle.

If radial coordinates are introduced as in (4.18) the hamiltonian becomes a function in radial phase space

$$H \rightarrow H(r,k,\ell^2) \qquad (5.2)$$

which defines a radial two-body scattering problem at a fixed angular momentum ℓ.

The radial equations are

$$\dot{r} = \{r,H\} = \frac{\partial H}{\partial k}$$

$$\dot{k} = \{k,H\} = -\frac{\partial H}{\partial r} \qquad (5.3)$$

In these equations the angular momentum appears as a parameter which can take any continuous value.

5.2. Radial phase space trajectories

The variational equations have now been reduced to what looks like an ordinary scattering problem in classical mechanics. There are however some important new features which are hidden in the transformation (4.10). The most obvious one we have discussed in section 4. in connection with the distortion and forbiddenness of regions in phase space. The other effect, of a dynamical nature, comes from the fact that, even for local two body forces, the hamiltonian (5.2) will be highly non-local except in the folding region. By no means the k dependence is through a mass term proportional to k^2. For the same reason the dependence on ℓ^2 will not appear as a centrifugal barrier ℓ^2/r^2. All these effects are important in what we have called the Pauli distorted region in radial phase space. Outside this region the hamiltonian takes the usual form

$$H(r,k,\ell^2) = \frac{\hbar^2}{2m\mu}(k^2 + \ell^2/r^2) + V_f(r)$$

where V_f is the folding potential.

Given an explicit form for H, we could easily solve the equations (5.3) to find $r(t)$, $k(t)$. It is, however much more interesting to use energy conservation to find the phase space trajectories $k(r)$. These are defined implicitly for given ℓ and E by

$$H(r,k,\ell^2) = E \qquad (5.4)$$

These trajectories have been plotted in Fig. 2 for α-α scattering. In Appendix B we give the details of the two body force and the oscillator parameter, which are the same as those used in ref[10]. The Coulomb force has been included in the folding approximation only, to produce results comparable to ref[10].

A word of caution should be raised here concerning the assignment of angular momentum. As our trial wave function does not have a well defined angular momentum, ℓ can adopt any real value. To assign the values with physical meaning we need an extra prescription. For large values of ℓ we can just choose ℓ to be integer. (Actually for α-α scattering one should choose ℓ as an even integer to take into account the identity of the fragments). That this procedure is not correct for small values of ℓ is well known from application of the WKB method to the radial Schrödinger equation[18]. In that case it is possible to show that ℓ should be chosen as

$$\ell = L_{QM} + \frac{1}{2} \qquad (5.5)$$

where L_{QM} takes on integer values and ℓ is the classical value of the angular momentum. This is also the prescription used when applying semiclassical methods to heavy ion reactions[19]. We have adopted this prescription here, although we have not been able to derive it. Its use is validated a posteriori by the excellent agreement with the quantum calculation in the next section. Obviously, the correct procedure to assign the angular momentum would be to use L-projected wave functions in the va-
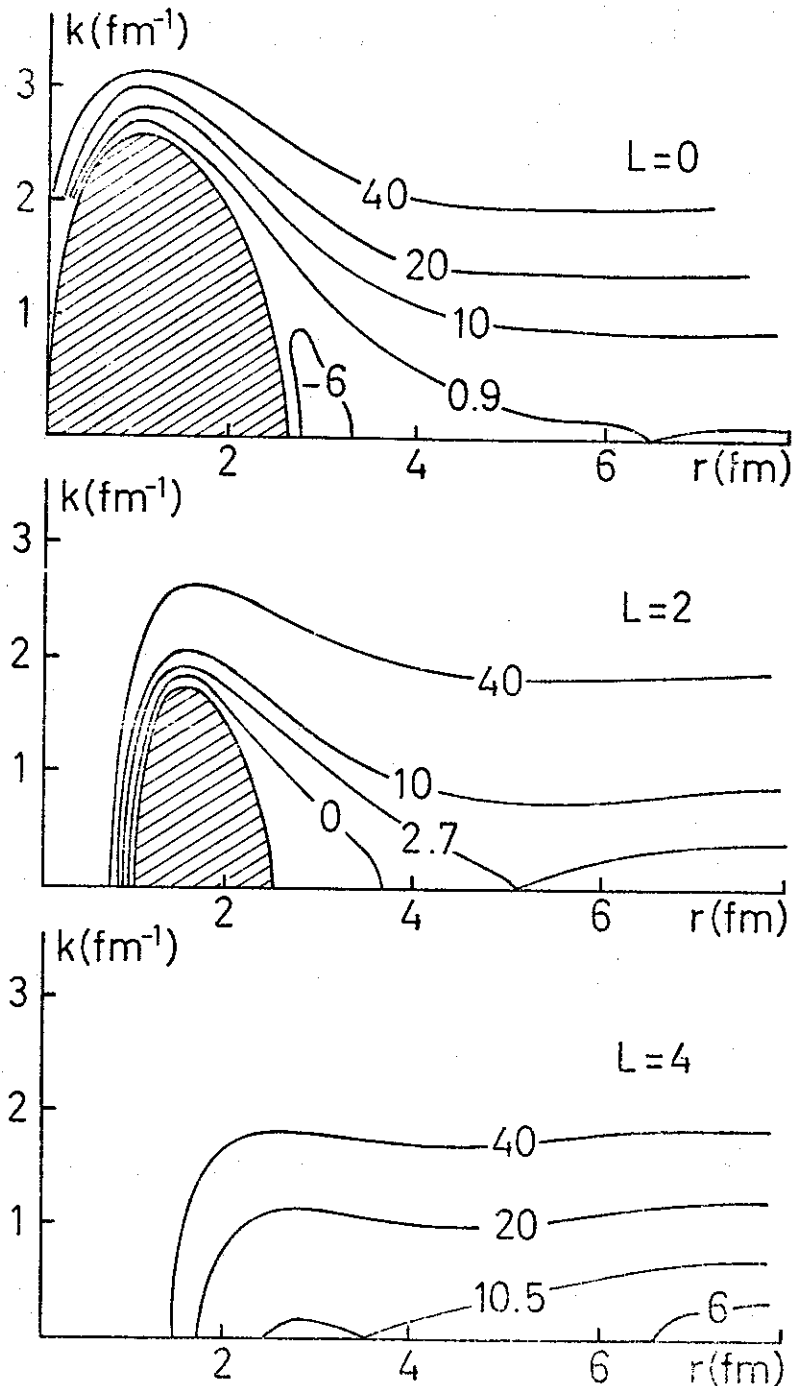
Figure 2 - Radial phase space trajectories for alpha-alpha scattering. The oscillator parameter is b = 1.37 fm. The trajectories are labeled by E_{CM} in MeV. The shaded region is forbidden and the dotted lines give the limit of the region of Pauli distortion (N_f=10). The angular momentum has been assigned by the prescription $\ell = L + 1/2$.

riational principle. This would lead to a classical hamiltonian $H_L(k,r)$ in which the continuous dependence on ℓ^2 is replaced by a discontinuous dependence on the allowed L-values. This problem needs further clarification.

In Fig. 2 the essential characteristics of α-α scattering can be recognized. In all cases we have drawn the critical trajectory leading to the top of the Coulomb barrier. This trajectory leads to orbiting of the fragments at a fixed distance and separates the trajectories which only feel the Coulomb repulsion from those that penetrate into the nuclear region. Notice that both the L=0 and L=2 barriers are well outside the distortion region indicated by the dotted line. This means that the barrier position and height is determined solely from the folding part of the potential. For L=4 instead the critical trajectory enters the Pauli distorted region and is therefore affected by antisymmetrization. Another interesting effect that can be seen clearly is how the periodic trajectories (cf. the small loop at -6 MeV for L=0) are strongly affected by antisymmetrization.

5.3. Computation of phase shifts

Semiclassically, in the WKB approximation, the nuclear phase shifts for two body scattering with a Coulomb plus nuclear potential are computed as[19]

$$\delta_L(E) = \int_{r_0}^{\infty} k \, dr - \int_{r_c}^{\infty} k_c \, dr \qquad (5.6)$$

where k and k_c are the wave numbers corresponding to the radial motion with and without the nuclear potential $U(r)$

$$k(r) = \left\{ \frac{2\mu m}{\hbar^2} \left[E - U(r) - V_c(r) \right] - (L + \tfrac{1}{2})^2/r^2 \right\}^{1/2}$$

$$(5.7)$$

$$k_c(r) = \left\{ \frac{2\mu m}{\hbar^2} \left[E - e^2 Z_1 Z_2/r \right] - (L + \tfrac{1}{2})^2/r^2 \right\}^{1/2}$$

Here r_o and r_c are the more outward turning points for the two trajectories, where k or k_c vanish, V_c is the Coulomb potential which at short distances could differ from the point Coulomb interaction $e^2 Z_1 Z_2/r$. The centrifugal potential is computed for the classical angular momentum $\ell = L + 1/2$.

In Fig. 3 we have represented the phase shift (5.6) schematically as an area in radial phase space. Disregarding for the moment the forbidden region (B+C) it is the area bounded between the curves k(r) and $k_c(r)$.

We propose to compute the phase shifts with a similar formula where k(r) is replaced by the trajectory obtained from the variational principle defined implicitly by (5.4). Examples of such trajectories are given in Fig. 2.

In the computation of the area under k(r) the forbidden region should be excluded. The second term in (5.6) is not modified. The resulting phase shift is again best characterized as an area in phase space. In Fig. 3 it is the area A-C.

In Fig. 4 we show the results of this computation and compare with the RGM results of ref[10]. The areas were evaluated dividing the phase plane in a grid of $\Delta k = 0.03$ fm^{-1} and $\Delta r = 0.06$ fm and adding the areas $\Delta r \Delta k$ that satisfied the condition of belonging to region A (counted positive) or C (counted negative). The accuracy of the procedure was checked in several instances by halving the size of the grid and verifying that the computed phase shifts did not change by more than one degree.

From Fig. 4 we conclude that the TDVP computation reproduces all the major features of the quantum one giving an overall quantitative agreement with RGM. Of course some features cannot be reproduced with the simple WKB formula (5.6). These features are connected with typically quantum phenomena like tunneling or reflection above the barrier. The semiclassical calculation has a discontinuity at the top of the Coulomb barrier where the classical trajectory suddenly enters the attraction region. This discontinuity is smoothed by tunneling effects in the RGM calculation. It is apparent from Fig.4 that both the position and the magnitude of the discontinuity are correctly given.
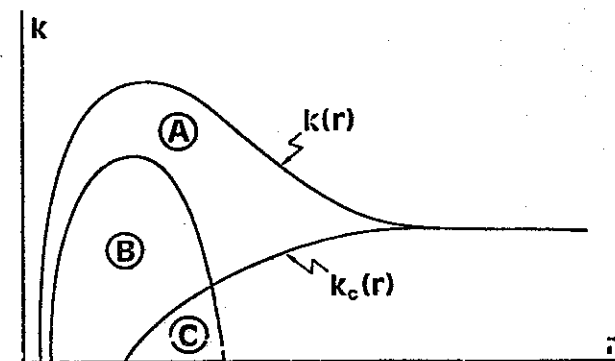
Figure 3 - Graphical computation of the semiclassical phase shift (schematic). The are B+C is forbidden. k(r) is the variational trajectory as given in Fig. 2. $k_c(r)$ is the Coulomb trajectory with the same energy and angular momentum. The nuclear phase shift is computed as the area A-C.
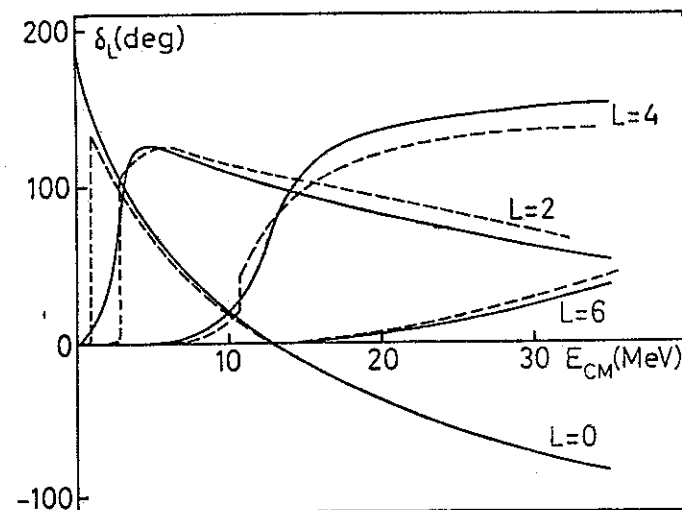

Figure 4 - Nuclear phase shifts for alpha-alpha scattering. Full line is the RGM calculation of ref[10]. Dotted lines are the results of this paper.

It is interesting to notice that the repulsive effect of antisymmetry (the "Pauli hard core") is accounted for by the negative contribution to the phase shift (area C in Fig.3) where the Coulomb trajectory enters the forbidden region.

Finnaly a brief comment on the computation of bound state energies. These would be naturally computed using the Bohr-Sommerfeld quantization condition on the closed periodic trajectories at negative energies. In the present case there is not enough area to hold a quantum state at negative energies and again this is due to the Pauli principle which acts by excluding area in phase space which could otherwise be occupied by a bound state. Although in the $\alpha-\alpha$ case it is not very relevant, it is appealing to know that for heavier systems, where one expects some bound states, the TDVP can provide a unified description of semiclassical type of bound states, phase shifts and even resonances (by extending the Sommerfeld rule to periodic trajectories at positive energies).

6. DISCUSSION AND CONCLUSIONS

We have presented a method based on the TDVP to study microscopically the scattering of light fragments. It borrows physical approximations and computational techniques from both TDHF and RGM-GCM. From TDHF it inherits the Slater determinant restriction to the wave function and the consequent one body evolution via the TDVP. However this evolution is not the more general one but is further constrained to allow only for the relative motion degree of freedom. On the other hand the method inherits from RGM-GCM the basic idea of clustering of nucleons and all the mathematical apparatus for the calculation of norm and overlap kernels. However it treats the RGM-GCM equations classically.

There are two main new results that we want to stress from the present work. The first is the concept that the effects of the Pauli principle between nuclear fragments can be assimilated to a distortion of the relative motion phase space and studied in a classical context. The main features of the quantum treatment of antisymmetrization via the eigenvalue problem

for the norm kernel are reproduced semiclassically including the forbidden and the partially forbidden states. Therefore, inasmuch as the radial motion of two fragments is semiclassical, there is no need for a full quantum treatment in order to include the effects of the Pauli principle. Of course, to fully substantiate this statement one would need more calculations for other pairs of nuclei. These are presently under way. Notice that, for heavier fragments, where the computation of the full overlap becomes very cumbersome we could consider expanding it according to the number of particles exchanged. Such expansions are well known[6,7] and using them one could study how the symplectic structure changes all the way from a "flat" phase space when no exchange is included to the full effects of antisymmetry. In any case, due to the strong optical absorption in the inner region and to the diminishing range of multiparticle exchange effects, only the first few terms of this expansion are expected to have significant influence on the scattering.

The second result that we want to stress is the possibility of extracting meaningful quantum information from a time dependent variational solution. This problem of re-quantization has been approached recently by many authors[20], but only in connection with bound state problems in simple models. We have shown here that in a fairly realistic situation these methods can be extended with success to scattering.

APPENDIX A

We provide here some details on the construction of the trial wave function and the proof that, for oscillator fragments, it can be chosen to depend analytically on a complex vector $\underline{s}$. We follow a simplified version of the methods proposed by Kramer, John, Schenzle[16] for the computation of overlap and hamiltonian kernels in the theory of interacting clusters.

A.1 - Weyl translation of a quantum state

Consider any normalizable single particle state $|\phi_0)$ and position and momentum operators $\hat{p}$, $\hat{q}$, such that $i[\hat{p},\hat{q}] = \hbar$. The Weyl translated state is defined as

$$|\phi_0(p,q)) = e^{\frac{i}{\hbar}(p\hat{q}-q\hat{p})} |\phi_0) = \hat{W}(p,q)|\phi_0) \qquad (A.1)$$

This state depends on the two c-numbers p, q and has the following properties

$$(\phi_0(p,q)|\hat{q}|\phi_0(p,q)) = (\phi_0|\hat{q}|\phi_0) + q$$
$$\qquad (A.2)$$
$$(\phi_0(p,q)|\hat{p}|\phi_0(p,q)) = (\phi_0|\hat{p}|\phi_0) + p$$

The interpretation is clear. If $|\phi_0)$ is a wave packet with given mean position and momentum, then $|\phi_0(p,q))$ is another wave packet shifted in phase space by the c-numbers p and q. All higher moments of $\hat{p}$ and $\hat{q}$ are unaffected. We can then think of $|\phi_0(p,q))$ as a state with a definite _mean_ position and momentum. Of course, in general it will not be an eigenstate of neither $\hat{p}$ nor $\hat{q}$. It is obvious that p and q can assume any value so that their ranges are

$$-\infty < p,q < \infty \qquad (A.3)$$

This argument only depends on the commutation relations of $\hat{p}$ and $\hat{q}$ so that it can be immediately generalized to the translation of the center of mass of many body wave functions. In fact, consider for a system of fermions the Slater determinant formed from A single particle wave functions $|\phi_i)$

$$<x|\psi> = \frac{1}{\sqrt{A!}} \det\{(x_i|\phi_j)\}$$

We use round brackets for single particle states and angle brackets for many body states. x_i labels the position, spin and isospin of particle i while x stands for the set $\{x_1,\ldots,x_A\}$. A Weyl shifted determinant is constructed as

$$<x|\psi_0(p,q)> = \frac{1}{\sqrt{A!}} \det\{(x_i|\phi_j(p,q))\}$$

and it is easy to see that it can be written as

$$|\psi_0(p,q)> = e^{\frac{i}{\hbar}\left[p\,\Sigma\hat{q}_i - q\,\Sigma\hat{p}_i\right]} |\psi_0>$$

Thus, in terms of the center of mass (CM) operators

$$\hat{Q} = \frac{1}{A} \sum_{i=1}^{A} \hat{q}_i \quad , \quad \hat{P} = \sum_{i=1}^{A} \hat{p}_i$$
$$\qquad (A.4)$$
$$i[\hat{P},\hat{Q}] = \hbar$$

we have

$$|\psi_0(p,q)> = e^{\frac{i}{\hbar}(Ap\,\hat{Q} - q\hat{P})} |\psi_0>$$

Then, in complete analogy with (A.1) and (A.2) we have

$$<\psi_0(p,q)|\hat{Q}|\psi_0(p,q)> = <\psi_0|\hat{Q}|\psi_0> + q$$

$$<\psi_0(p,q)|\hat{P}|\psi_0(p,q)> = <\psi_0|\hat{P}|\psi_0> + pA$$

It is then convenient to label the many-body state by the mean values of the CM operators as

$$|\psi_0(P,Q)> = e^{\frac{i}{\hbar}(P\hat{Q}-Q\hat{P})} |\psi_0> \qquad (A.5)$$

where

$$P = Ap \quad , \quad Q = q \qquad (A.6)$$

This is the relationship between the Weyl shifts of the single particle states and the phase space coordinates of the fragment.

A.2- Complex form of the Weyl operator

When the single particle states are oscillator states it is more convenient to rewrite the Weyl operator in terms of creation and annihilation operators

$$\hat{a}^{\dagger} = \frac{1}{\sqrt{2}} \left(\frac{\hat{q}}{b} - i \frac{b\hat{p}}{\hbar} \right)$$

(A.7)

$$\hat{a} = \frac{1}{\sqrt{2}} \left(\frac{\hat{q}}{b} + i \frac{b\hat{p}}{\hbar} \right)$$

$$[a,a^{\dagger}] = 1$$

and the complex variables

$$\bar{z} = \frac{1}{\sqrt{2}} \left(\frac{q}{b} + i \frac{bp}{\hbar} \right)$$

(A.8)

$$z = \frac{1}{\sqrt{2}} \left(\frac{q}{b} - i \frac{bp}{\hbar} \right)$$

In the above formulae $b = \sqrt{\hbar/m\omega}$ is the oscillator lenght of a particle of mass m in an oscillator of frequency ω. Using (A.7) and (A.8) the Weyl shift operator can be written in complex form

$$\hat{W}(p,q) = \hat{W}_c(z,\bar{z}) = e^{\bar{z}\hat{a}^{\dagger} - z\hat{a}}$$

(A.9)

The Baker-Hausdorff formula can be used to write (A.9) in the alternative forms

$$\hat{W}_c(z,\bar{z}) = e^{-\frac{1}{2} z\bar{z}} e^{z\hat{a}^{\dagger}} e^{-z\hat{a}} = e^{\frac{1}{2} z\bar{z}} e^{-z\hat{a}} e^{\bar{z}\hat{a}^{\dagger}}$$ (A.10)

A special but very important case occurs when we let this operator act on the ground state of the oscillator, defined by $\hat{a}|0) = 0$. In this case, using (A.10) we obtain

$$\hat{W}_c(z,\bar{z})|0) = e^{-\frac{1}{2} z\bar{z}} e^{\bar{z}\hat{a}^{\dagger}} |0)$$

Notice that, except for the normalization factor $e^{-\frac{1}{2} z\bar{z}}$, we obtain a state parametrized analytically in terms of the complex variable $\bar{z}$. It is, of course, the usual coherent state of the harmonic oscillator.

A.3 - Trial wave function for two fragments

It is quite natural to try to describe a scattering situation for two fragments of masses A_1 and A_2 by the anti-symmetrized product of two Weyl translated states

$$|\underline{P}_1,\underline{Q}_1,\underline{P}_2,\underline{Q}_2> = A\{W_1(\underline{P}_1,\underline{Q}_1)|\psi_1> W_2(\underline{P}_2,\underline{Q}_2)|\psi_2>\}$$ (A.11)

where A is the antisymmetrization operator and $|\psi_1>$ and $|\psi_2>$ are Slater determinants constructed from single particle states $|i_1>$, $i_1 = 1,\ldots,A_1$ and $|i_2>$, $i_2 = 1,\ldots,A_2$.

We will assume that states in each fragment are orthonormal

$$(i_1|i_1') = \delta_{i_1 i_1'}$$

$$(i_2|i_2') = \delta_{i_2 i_2'}$$

For the moment, states $|i_1)$ need not be the same as $|i_2)$.

We now transform to center of mass and relative coordinates in the usual way

$$\hat{\underline{Q}}_{CM} = \frac{A_1\hat{\underline{Q}}_1 + A_2\hat{\underline{Q}}_2}{A_1+A_2} = \frac{1}{A_1 + A_2} \sum_{i=1}^{A} \hat{\underline{q}}_i$$

$$\hat{\underline{P}}_{CM} = \hat{\underline{P}}_1 + \hat{\underline{P}}_2 = \sum_{i=1}^{A} \hat{\underline{p}}_i$$

(A.12)

$$\hat{\underline{P}} = \frac{A_2\hat{\underline{P}}_1 - A_1\hat{\underline{P}}_2}{A_1 + A_2} = \frac{A_2}{A} \sum_{i \in 1} \hat{\underline{p}}_i - \frac{A_1}{A} \sum_{i \in 2} \hat{\underline{q}}_i$$

$$\hat{\underline{Q}} = \hat{\underline{Q}}_1 - \hat{\underline{Q}}_2 = \frac{1}{A_1} \sum_{i \in 1} \hat{\underline{q}}_i - \frac{1}{A_2} \sum_{i \in 2} \hat{\underline{q}}_i$$

with similar formulas for the c-numbers $\underline{Q}_1$, $\underline{P}_1$, $\underline{Q}_2$, $\underline{P}_2$. The trial state can then be rewritten as

$$|\underline{P}_{CM}, \underline{Q}_{CM}, \underline{P}, \underline{Q}> = \hat{W}_{CM}(\underline{P}_{CM}, \underline{Q}_{CM}) \; A\left[\hat{W}(\underline{P},\underline{Q})|\psi_1>|\psi_2>\right] \tag{A.13}$$

As the CM operators are symmetric under particle exchange we have commuted them with the antisymmetrizer. This of course cannot be done with the relative motion operators $\hat{\underline{P}}$, $\hat{\underline{Q}}$.

The Weyl shift corresponding to the CM coordinates is relatively uninteresting as we deal usually with translation and Galileian invariant hamiltonians. When the single particle states are harmonic oscillator the CM coordinate factors as a product wave function and the CM motion is completely separated from the relative motion. In other cases projection techniques are available but we will not deal with such cases here. We therefore concentrate on the relative motion wave function. Using (A.12) we can rewrite it as

$$|\underline{P},\underline{Q}> = A\left[e^{\frac{i}{\hbar}(\underline{P}\cdot\hat{\underline{Q}}-\underline{Q}\cdot\hat{\underline{P}})}|\psi_1>|\psi_2>\right] =$$

$$= A\left[e^{\frac{i}{\hbar}(\underline{P}\cdot\hat{\underline{Q}}_1 - \frac{A_2}{A_1+A_2}\underline{Q}\cdot\hat{\underline{P}}_1)}|\psi_1> \; e^{\frac{i}{\hbar}(\underline{P}\cdot\hat{\underline{Q}}_2 - \frac{A_1}{A_2+A_1}\underline{Q}\cdot\hat{\underline{P}}_2)}|\psi_2>\right]$$

Then the relative motion wave function is built up from single particle states

$$e^{\frac{i}{\hbar}A_1^{-1}(\underline{P}\cdot\hat{\underline{q}} - \mu\underline{Q}\cdot\hat{\underline{p}})}|i_1) \quad \text{in fragment 1}$$

$$e^{-\frac{i}{\hbar}A_2^{-1}(\underline{P}\cdot\hat{\underline{q}} - \mu\underline{Q}\cdot\hat{\underline{p}})}|i_2) \quad \text{in fragment 2} \tag{A.14}$$

where we have introduced the relative mass number

$$\mu = \frac{A_1 A_2}{A_1+A_2} \tag{A.15}$$

If we use the single particle boson operators introduced in (A.7) we obtain the complex form of (A.14)

$$\exp\left[\frac{\sqrt{\mu}}{A_1}(\underline{\bar{s}}\cdot\hat{\underline{a}}^\dagger - \underline{s}\cdot\hat{\underline{a}})\right]|i_1) \quad \text{in fragment 1}$$

$$\exp\left[-\frac{\sqrt{\mu}}{A_2}(\underline{\bar{s}}\cdot\hat{\underline{a}}^\dagger - \underline{s}\cdot\hat{\underline{a}})\right]|i_2) \quad \text{in fragment 2} \tag{A.16}$$

The complex vector $\underline{s}$ is related to $\underline{P}$ and $\underline{Q}$ by

$$\underline{s} = \frac{1}{\sqrt{2}}\left[\frac{\sqrt{\mu}}{b}\underline{Q} - i\frac{b}{\hbar\sqrt{\mu}}\underline{P}\right] \tag{A.17}$$

In general the Slater determinant constructed with the states (A.16) depends non-analytically on $\underline{s}$, i.e. it has a functional dependence on both $\underline{s}$ and $\underline{\bar{s}}$. However if the states $|i_1)$ and $|i_2)$ are oscillator states with the same parameter b it is easy to show that the essential dependence is on $\underline{\bar{s}}$ and that the dependence on $\underline{s}$ is only through an overall factor. In view of the properties of the variational principle discussed in Section 2. we can just drop this factor and obtain an analytical parametrization. To prove this statement we use (A.10) to write

$$e^{\underline{\bar{s}}_1\cdot\hat{\underline{a}}^\dagger - \underline{s}_1\cdot\hat{\underline{a}}}|i_1) = e^{-\frac{1}{2}\underline{s}_1\cdot\underline{\bar{s}}_1} e^{\underline{\bar{s}}_1\cdot\hat{\underline{a}}^\dagger} e^{-\underline{s}_1\cdot\hat{\underline{a}}}|i_1) =$$

$$= e^{-\frac{1}{2}\underline{s}_1\cdot\underline{\bar{s}}_1} \sum_{i_1'} e^{\underline{\bar{s}}_1\cdot\hat{\underline{a}}^\dagger}|i_1')(i_1'|e^{-\underline{s}_1\cdot\hat{\underline{a}}}|i_1) \tag{A.18}$$

Here we have introduced $\underline{s}_1 = \mu^{1/2}/A_1\underline{s}$ and inserted a complete set of oscillator states which is truncated at the maximum occupation number in the fragment. The Weyl translated states in fragment 1 are then linear combinations of the states $e^{\underline{\bar{s}}_1\cdot\hat{\underline{a}}^\dagger}|i_1)$ which are much easier to handle and depend analytically on $\underline{\bar{s}}$. The transformation matrix $(i_1'|e^{-\underline{s}\cdot\hat{\underline{a}}}|i_1)$ is lower triangular with unit diagonal and therefore its determinant is one. This means that the determinant constructed with the states

$$e^{\underline{\bar{s}}_1\cdot\hat{\underline{a}}^\dagger}|i_1) \quad \text{in fragment 1}$$

$$e^{-\underline{\bar{s}}_2\cdot\hat{\underline{a}}^\dagger}|i_2) \quad \text{in fragment 2} \tag{A.19}$$

is the same as the one constructed with the states

$$e^{\bar{s}_1 \cdot \hat{a}^\dagger} \; e^{-s_1 \cdot \hat{a}} \; |i_1) \quad \text{in fragment 1}$$

$$\qquad (A.20)$$

$$e^{-\bar{s}_2 \cdot \hat{a}^\dagger} \; e^{s_2 \cdot \hat{a}} \; |i_2) \quad \text{in fragment 2}$$

The argument is not valid if the fragments are excited. The only source of non-analyticity is the multiplying factor in (A.18) which we drop from now on.

Our main conclusion is then that it is possible to describe two oscillator clusters in relative motion with a trial wave function that depends analytically on a complex vector $\underline{s}$. In the main text we denote this wave function as

$$|\underline{s}\rangle = \left[\prod_{i_1=1}^{A_1} e^{\bar{s}_1 \cdot \hat{a}^\dagger} |i_1) \; \prod_{i_2=1}^{A_2} e^{-\bar{s}_2 \cdot \hat{a}^\dagger} |i_2) \right]$$

$$\qquad (A.21)$$

where

$$\underline{s}_1 = \frac{\mu^{1/2}}{A_1} \underline{s} \;, \quad \underline{s}_2 = \frac{\mu^{1/2}}{A_2} \underline{s} \qquad (A.21a)$$

and where $\underline{s}$ is related to $\underline{P}$ and $\underline{Q}$ by (A.17).

A.4 - Computation of the overlap $\langle s|s\rangle$

It is well known[21] that the overlap of two Slater determinants is given by the determinant of the matrix of overlaps which also plays a fundamental role in the computation of mean values of one and two body operators. For our purposes the overlap matrix B is conveniently partitioned in blocks

$$B = \begin{pmatrix} B^{11} & B^{12} \\ B^{21} & B^{22} \end{pmatrix}$$

where $B^{\alpha\beta}$ $\alpha, \beta = 1,2$ are the overlaps of the single particle states (A.20). Using repeatedly the decomposition (A.10) we compute explicitly the B blocks

$$B^{11} = \delta_{i_1 i_1'} \; e^{\underline{s}_1 \cdot \bar{\underline{s}}_1}$$

$$B^{12} = e^{-\underline{s}_1 \cdot \bar{\underline{s}}_2} \; (i_1 | e^{-\mu^{1/2} \bar{\underline{s}} \cdot \hat{a}^\dagger} \; e^{-\mu^{1/2} \underline{s} \cdot \hat{a}} \; |i_2)$$

$$B^{21} = (B^{12})^+$$

$$B^{22} = \delta_{i_2 i_2'} \; e^{\underline{s}_2 \cdot \bar{\underline{s}}_2}$$

Because the diagonal blocks are proportional to unit matrices the determinant is easily computed using the matrix identity

$$B = \begin{pmatrix} B^{11} & 0 \\ 0 & B^{22} \end{pmatrix} \begin{pmatrix} 1 & (B^{11})^{-1}B^{12} \\ 0 & 1 \end{pmatrix} \begin{pmatrix} 1-(B^{11})^{-1}B^{12}(B^{22})^{-1}B^{21} & 0 \\ 0 & 1 \end{pmatrix} \begin{pmatrix} 1 & 0 \\ (B^{22})^{-1} B^{21} & 1 \end{pmatrix}$$

Explicit computation yields then the final result

$$\langle \underline{s}|\underline{s}\rangle = e^{\underline{s} \cdot \bar{\underline{s}}} \; \det\left[1 - M^{12}(M^{12})^+ \; e^{-\underline{s} \cdot \bar{\underline{s}}/\mu} \right] \qquad (A.23)$$

where

$$M^{12} = (i_1 | e^{-\mu^{-1/2} \bar{\underline{s}} \cdot \hat{a}^\dagger} \; e^{\mu^{-1/2} \underline{s} \cdot \hat{a}} \; |i_2) \qquad (A.24)$$

This is a very compact and easy to use expression for the overlap. The interpretation is also quite simple. The first factor is what we would obtain if we were to neglect antisymmetrization. In that case the trial wave function is a coherent state in the relative coordinates and $e^{\underline{s} \cdot \bar{\underline{s}}}$ is the familiar overlap of two coherent states. The second factor in (A.23) reflects the influence of antisymmetrization. Notice that it is given as a determinant of a matrix with the dimension of the number of particles in the smaller fragment. Its computation is then quite manageable. The matrix $M^{12}(M^{12})^+$ has as elements finite polynomials in s and $\bar{s}$ and its computation is lenghty but straightforward. The negative exponential $e^{-\underline{s} \cdot \bar{\underline{s}}/\mu}$ takes into account the decreasing influence of the Pauli principle as $\underline{s} \cdot \bar{\underline{s}}$ becomes large.

To conclude we give explicit formulas for some pairs of fragments of interest

$\alpha-\alpha$ $(\mu=2)$

$$\langle \underset{\sim}{s}|\underset{\sim}{s}\rangle = e^{\underset{\sim}{s}\cdot\bar{\underset{\sim}{s}}}\left[1 - e^{-x}\right]^4 \qquad (A.25)$$

$\alpha-^{16}O$ $(\mu = 16/5)$

$$\langle \underset{\sim}{s}|\underset{\sim}{s}\rangle = e^{\underset{\sim}{s}\cdot\bar{\underset{\sim}{s}}}\left[1 - (1+x)\ e^{-x}\right]^4 \qquad (A.26)$$

$\alpha-^{40}Ca$ $(\mu = 40/11)$

$$\langle \underset{\sim}{s}|\underset{\sim}{s}\rangle = e^{\underset{\sim}{s}\cdot\bar{\underset{\sim}{s}}}\left[1 - (1 + x + \tfrac{1}{2}x^2)e^{-x}\right]^4 \qquad (A.27)$$

$^{16}O - ^{16}O$ $(\mu = 8)$

$$\langle \underset{\sim}{s}|\underset{\sim}{s}\rangle = e^{\underset{\sim}{s}\cdot\bar{\underset{\sim}{s}}}\left[1 - (4 + x^2)e^{-x} + (6 + 2x^2)e^{-2x} - \right.$$
$$\left. - (4 + x^2)\ e^{-3x} + e^{-4x}\right]^4 \qquad (A.28)$$

where we have used $x = \dfrac{\underset{\sim}{s}\cdot\bar{\underset{\sim}{s}}}{\mu}$.

In all cases the 4th power is due to the fact that the fragments are spin-isospin saturated. The simple dependence on only the quantity $\underset{\sim}{s}\cdot\bar{\underset{\sim}{s}}$ is due to the fact that the fragments are SU(3) scalars.

APPENDIX B

We collect here the details and analytic form of the hamiltonian kernel for $\alpha-\alpha$ scattering.

a) The two body interaction

The hamiltonian for the relative motion (with CM energy subtracted) is

$$H = T_{rel} + V + V_{coul}$$

$$T_{rel} = \frac{1}{2A} \sum_{i\neq j}^{A} \frac{(\underset{\sim}{p}_i - \underset{\sim}{p}_j)^2}{2m}$$

$$V = \frac{1}{2} \sum_{i\neq j}^{A} v(r_{ij})$$

where

$$v(r) = V_0(W + MP_x + BP_\sigma + HP_xP_\sigma)e^{-\beta r^2}$$

The parameters are in complete agreement with ref[10] and are $\beta = 0.46\ fm^{-2}$, $V_0 = -72.98$ MeV, $W = 0.3742$, $M = 0.4408$, $B = 0.1159$, $H = 0.0691$. They correspond to a mixture of 94% Serber + 6% Rosenfeld force.

b) The hamiltonian kernel

Matrix elements of one and two body operators in Slater determinant states built from non orthogonal single particle states can be calculated using the techniques of ref.[6]. For the $\alpha-\alpha$ case the methods of ref.[21] are simpler. The resulting analytic expressions are

$$H(\underset{\sim}{s},\bar{\underset{\sim}{s}}) = \tau + V + V_{coul}$$

$$\tau(\underline{s},\underline{\bar{s}}) = \frac{\langle \underline{s}|T_{rel}|\underline{s}\rangle}{\langle \underline{s}|\underline{s}\rangle} = \hbar\omega \left[\frac{21}{4} - \frac{(\underline{s}-\underline{\bar{s}})^2}{4} + \frac{\underline{s}\cdot\underline{\bar{s}}\;E}{1-E} \right]$$

$$V(\underline{s},\underline{\bar{s}}) = \frac{\langle \underline{s}|V|\underline{s}\rangle}{\langle \underline{s}|\underline{s}\rangle} = X_d\,V_d + X_e\,V_e$$

where

$$X_d = 8W + 4B - 4H - 2M$$

$$X_e = 8M + 4H - 4B - 2W$$

$$V_d = K_0 \left\{ 1 + I(\underline{s}+\underline{\bar{s}}) + \right.$$

$$\left. + \frac{\left[I(\underline{s}-\underline{\bar{s}}) - I(\underline{s}+\underline{\bar{s}})\right]E^2 - 2\left[I(\underline{s}) + I(\underline{\bar{s}}) - 1 - I(\underline{s}+\underline{\bar{s}})\right]E}{(1-E)^2} \right\}$$

$$V_e = K_0 \left\{ 1 + \frac{\left[I(\underline{s}+\underline{\bar{s}}) + 2 - 2I(\underline{s}) - 2I(\underline{s})\right]E}{(1-E)^2} \right\}$$

$$K_0 = 2V_0 \left[1 + 2/(b^2\beta)\right]^{-3/2}$$

$$I(\underline{x}) = \exp\left[-\frac{1}{4}\frac{\beta b^2}{1+2\beta b^2}\underline{x}^2\right]$$

$$E = \exp\left[-\frac{1}{2}\underline{s}\cdot\underline{\bar{s}}\right]$$

In the final calculations the constant terms in V and τ yielding the ground state energy of the separated alphas, were subtracted.

The Coulomb interaction was calculated neglecting antisymmetrization as

$$V_c \sim \int \rho\left(\underline{r}_1 - \frac{R}{2}\right) \frac{e^2}{|\underline{r}_1-\underline{r}_2|} \rho\left(r_2 + \frac{R}{2}\right) d\underline{r}_1\, d\underline{r}_2$$

where ρ is the density distribution of each fragment. Normalizing to the point Coulomb interaction at large distances we obtain

$$V_c(|\underline{Q}|) = \frac{4e^2}{|\underline{Q}|} \mathrm{erf}\left[\frac{|\underline{Q}|}{\sqrt{2}\,b}\right]$$

c) The folding limit

In both V and τ a leading term can be isolated which dominates asymptotically for $\underline{s}\cdot\underline{\bar{s}} \to \infty$. In this limit the hamiltonian becomes

$$H \to H_f = -\frac{1}{4}\hbar\omega(\underline{s}-\underline{\bar{s}})^2 + X_d K_0 I(\underline{s}+\underline{\bar{s}})$$

which in terms of $\underline{P}$ and $\underline{Q}$ takes the folding form

$$H_f = \frac{1}{2m\mu}\underline{P}^2 + V_f(|\underline{Q}|) + V_c(|\underline{Q}|)$$

where

$$V_f(|\underline{Q}|) = X_d K_0 \exp\left[-\frac{\beta Q^2}{1+2\beta b^2}\right]$$

This is the form of the hamiltonian outside the distorted region. It has a local gaussian form for the potential and a kinetic energy with the (constant) reduced mass.

REFERENCES

1. P.A.M.Dirac, Proc.Camb.Phil.Soc. 26 (1930) 376.

2. J.W.Negele, "The Mean field Theory of Nuclear Structure and Dynamics", Massachussets Institute of Tecnology report CTP 898 (1981).

3. K.T.R.Davies, K.R.S.Devi, S.E.Koonin , M.R.Strayer, TDHF Calculations of Heavy-Ion Collisions, Marmal Aid Preprint Series MAP-23 (1982).

4. K.Wildermuth, Y.C.Tang, A Unified Theory of the Nucleus, (Vieweg, Braunschweig, 1977).
   Y.C. Tang, M.LeMere, D.R.Thompson, Phys. Rep. 47 (1978) 167.

5. D.L.Hill, J.A.Wheeler, Phys.Rev. 89 (1953) 1102.
   J.J.Griffin, J.A.Wheeler, Phys. Rev. 108 (1957) 311.
   C.W.Wong, Phys. Rep. 15 (1975) 283.

6. P.Kramer, G.John, D.Schenzle, Group Theory and the Interaction of Composite Nucleon Systems, (Vieweg, Braunschweig, 1981).

7. H.Horiuchi, Prog.Theor.Phys.Suppl. 62 (1977) 90.

8. S.Drozdz, J. Okolowicz, M.Ploszajczak, Phys. Lett. 109 B (1982) 150.

9. E.Courier, B.Grammaticos, T.Sami, Phys.Lett. 109 B (1982) 145.

10. S.Okai, S.C.Park, Phys. Rev. 143 (1966) 787.

11. P.Kramer, M.Saraceno, "Geometry of the Time Dependent Variational Principle in Quantum Mechanics", Lecture Notes in Physics Vol. 140 (Springer Verlag, Berlin, 1981).

12. A.K.Kerman, S.E.Koonin, Annals of Physics 100 (1976) 332.

13. P.C.Lichtner, J.J.Griffin, H.Schultheis, R.Schultheis, A.B.Volkov, Phys. Lett. 88 B, (1979) 221.

14. H.Goldstein, "Classical Mechanics", (Addison-Wesley, Massachusetts, 1950).

15. J.P.Elliott, T.H.Skyrme, Proc. Roy. Soc. A232 (1955), 561.

16. V.I. Arnold, Mathematical Methods of Classical Mechanics, (Springer Verlag, New York, 1978), p. 230.

17. G.R.Satchler, W.G.Love, Phys.Rep. 55 (1979) 183.

18. R.E.Langer, Phys.Rev. 51 (1937) 669.

19. D.M.Brink, in Nuclear Physics with Heavy Ions and Mesons, ed R.Balian, M.Rho, G.Ripka Vol. 1 (North Holland, Amsterdam, 1978) p. 1.

20. K.K.Kan, J. J. Griffin, P.C.Lichtner, M.Dworzecka, Nucl. Phys. A332 (1979) 109.
    S.Levit, J. W. Negele, Z. Paltiel, Phys. Rev. C21 (1980) 1603.
    H.Kuratsuji, Phys. Lett. 108B (1982) 367.

21. D.Brink, Rend. della XXXVI Scuola Enrico Fermi, ed. C. Bloch (Academic Press, New York, 1966) p. 247.